

Mechatronic Design and Robust Control of an Artificial Ventilator in Response to the COVID-19 Pandemic

Serafin Ramos-Paz, Rubén Belmonte-Izquierdo, Luis Alfonso Inostroza-Moreno
Luisa Fernanda Velasco-Rivera, Ricardo Mendoza-Villa and Valeria Gaona-Flores
Instituto Tecnológico y de Estudios Superiores de Monterrey
School of Science and Engineering, Mechatronics Engineering Department
Avenida Montaña Monarca 1340, Ejido Jesús del Monte
Morelia, Michoacán México, 58350
serafin.ramos.paz@tec.mx

Abstract—

The crisis resulting from the COVID-19 pandemic has generated an adverse situation in which thousands of people dies due to the lack of artificial ventilation devices. In this sense, this work presents a proposal for the robust mechatronic design and control of a low-cost non-invasive ventilator, for which rapid prototyping manufacture strategies such as 3D printing and product design are used. In order to guarantee the reliability of the system operation, in this work, a robust control scheme based on super-twisting sliding modes is proposed, which guarantees the trajectory tracking control corresponding to the breathing profiles required by the patients. Experimental and simulation results validate the effectiveness of the proposed prototype design. Nevertheless, the prototype is waiting to be tested and approved for use in health assistance.

I. INTRODUCTION

The coronavirus pandemic is a major health emergency, as of 15 July, the World Health Organization (WHO) has reported over 1.3 Million of confirmed coronavirus cases all over the world. According to data provided by WHO, 80% of confirmed coronavirus cases will be able to recover without the need for hospitalization. However, 1 in 6 patients could have significant aggravated symptoms, causing damage to the lungs and therefore decreasing the levels of oxygen in the body. In this sense for patients with severe effects of the infection, an artificial ventilator may offer the best chance of survival [1]. Since 1990, the interest in providing positive pressure ventilation (PPV) through a mask rather than through an endotracheal tube has increased. This method has been called non-invasive ventilation NIV [2], since the patient is not intubated, NIV has certain potential advantages compared with invasive ventilation methods. NIV is relatively easy to apply and can be used for short intervals because it can be started and stopped very easily and the major advantage of avoiding the complications associated with intubation and they are usually more comfortable for the patients

reducing the need for anesthesia required for intubation [3]. In recent works it is possible to find developments of artificial ventilators as full-professional devices [4]–[6], nonetheless, different efforts have been done in order to develop low-cost artificial ventilators as seen in [7], [8], and due to the COVID-19 pandemic, the efforts for developing a low-cost ventilator have increased significantly because of the lack of this devices within the public health institutions. One of the possible solutions for the development of an artificial ventilator is the conditioning of existing technology, such as the case of airway mask units (AMBU) [9], which are devices for manual artificial ventilation, that can be automated by using adequate mechanisms and control systems.

In this sense, this paper leads to the mechatronic design and robust control of a low-cost artificial ventilator, in response to the COVID-19 pandemic. The proposed design is mainly based on the automated regulation of the tidal volume flow, required during the respiratory cycle, which is generated through the compression of an AMBU, due to the motion generated by a slider-crank mechanism [10] which tracks a desired respiratory profile. Therefore the regulation of the compression cycle of the AMBU becomes a problem of trajectory tracking control, which is achieved for the purposes of this paper, through sliding modes super-twisting robust control strategy. When designing control schemes for devices in which ensuring their operation and the reliability of their operation becomes a critical issue, it is necessary to implement some robust control schemes. Among the most popular robust control schemes are PID-type controllers [11], which are considered robust in the sense of rejecting disturbances and not depending on the mathematical model of the system, and only on an error signal and proper tuning of the controller, which can be done even by heuristic methods. However, there are certain limitations for this type of controllers, such as the linear regions of operation and the inability of a PID-type controller to track time-varying signals. In this sense, in this work, the use of a control

scheme based on sliding modes and its super-twisting variant is proposed.

The proposed artificial ventilator mechatronic design has the following practical advantages: a) a non-invasive mechanical ventilator, reducing the risk derived for the use of anesthesia during invasive intubation. b) low-cost design based on rapid prototyping technologies such as 3D printing, c) the simplicity of the mechanical system based on a slider-crank mechanism, and an airway mask bag unit (AMBU), d) a robust controller capable of performing trajectory tracking control to follow the desired respiratory profiles. The aforementioned practical advantages of the proposed design are considered to be the main contributions of this paper.

The structure of the paper is as follows: Section II describes the mechatronic design of the mechanical ventilator. Section III describes the nonlinear robust control based on super-twisting sliding modes that will be used for the proposed application. Experimental results are presented in Section IV, and finally, Section V presents the conclusions about this work.

II. ARTIFICIAL VENTILATOR DESIGN

In this section, the basis of mechanical ventilation is exposed. Then based on the general understanding of the requirements of the mechanical ventilation issue, the mechatronic design of the system is presented, based on the electrical and mechanical modeling of the components of the system.

A. Breathing Process Description

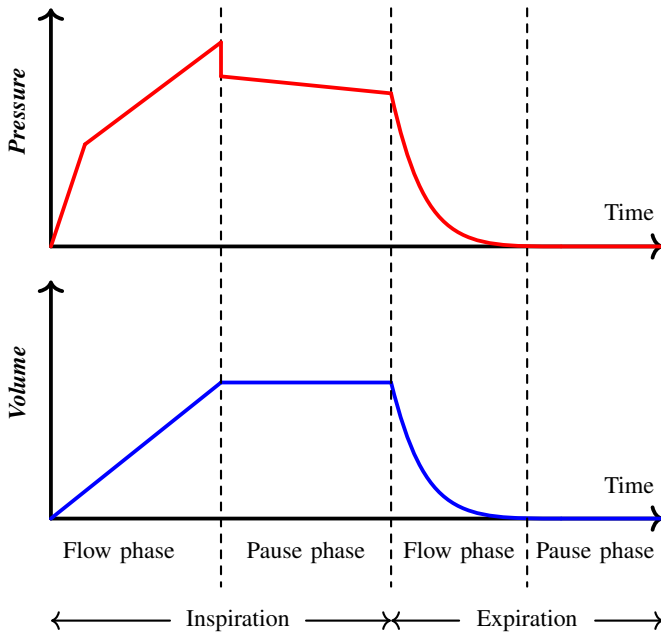


Fig. 1: Typical Ventilation Cycle.

The artificial ventilation process consists of a periodical behavior of filling and evacuating the lungs, this process is

carried out by the proper control of an artificial ventilator by following the ventilation cycle as seen in Fig. 1. The respiratory cycle consists of an expiration phase, an inspiration phase, and a pause phase. During the resting phase, the expiratory muscles are at rest, the diaphragm does not contract, air does not enter or exit, and the three chest diameters are anatomically positioned. In the anatomical position, the pressure inside the lungs is going to be equal to the atmospheric pressure. The inspiration phase begins with a contraction of the diaphragm and all the inspiratory muscles and an increase in the three chest diameters occurs in such a way that inside the lungs, the intrapulmonary volume increases. In the inspiratory phase, a negative pressure is created in the lungs, which will facilitate the entry of air into the lungs. The lung is insufflated, it is filled with air until a moment comes that reaches its maximum degree of extensibility, the alveolar walls become rigid, because they do not allow to elongate more and an elastic retraction force appears, and at that moment the phase begins expiration, in which this retraction force that is generated will decrease the three diameters, generating a positive pressure that will cause the air to be expelled.

B. How does a ventilator works

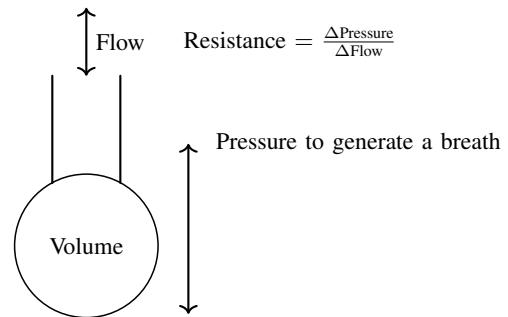


Fig. 2: Respiratory System .

The movement of air from outside the body into the lungs and vice versa is ensured by means of a pressure gradient between the exterior pressure (P_{atm}) and the alveolar pressure (P_{alv}), which is the pressure between the lungs. For mechanical ventilation two scenarios are of interest: On the one hand if P_{alv} decreases with respect to P_{atm} , this case is called negative pressure ventilation, which is the natural breathing condition, and on the other hand if P_{atm} increases with respect to P_{alv} , this condition is called positive pressure ventilation (which is the scenario during mechanical ventilation), the greater the flow the greater the pressure and as a consequence, for the same flow if the resistance increases the pressure rises. Consider the breathing diagram as seen in Fig. 2, the expansion of an elastic bag is produced by the so-called transpulmonary pressure which is the difference between P_{alv} and the pleural pressure (P_{pl}) that is the pressure generated between the lungs and the thoracic cage. The force exerted during mechanical ventilation is the sum of the pressure generated by the patient muscles and the pressure

generated by the ventilator [2]. Different control objectives can be achieved during mechanical ventilation as they are the volume-control or pressure-control mode. During the volume control ventilation, the desired tidal volume and respiratory rate are defined by the user and the airways pressure is the dependent variable dependent on the mechanical properties of the patient respiratory system [3]. Therefore the main task of a ventilator is to transform energy into one of the output variables such as flow, pressure, or volume, this results in a control objective of regulating the positive pressure applied to the airways or the sub-atmospheric pressure to the exterior of the chest.

C. Mechatronic Design

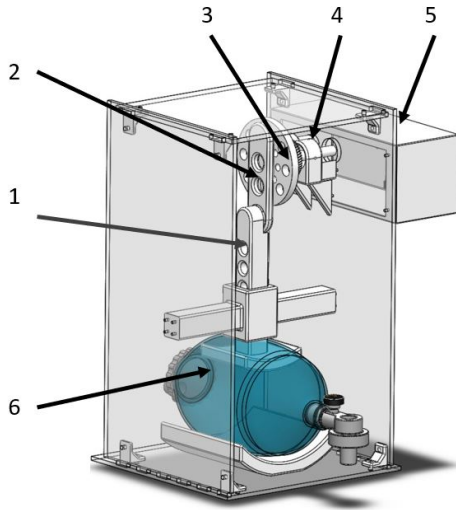


Fig. 3: Artificial breathing machine CAD protipe, designed using Dassault Systemes Solidworks®. 1. slider link, 2. connecting rod, 3. crank, 4. gearbox, 5. control box, 6. AMBU.

Our proposal for a ventilator is based on a slider-crank mechanism, which can be seen in Fig. 3. This mechanism is composed by three parts pointed out as components from 1 to 3 in Fig. 3, these are the slider, connecting rod, and the crank respectively. The motion is generated by means of a 12V DC motor connected to a gearbox system, which transmits power and enough torque to compress the AMBU bag with the lower part of the slider.

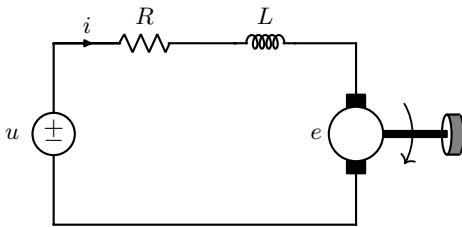


Fig. 4: DC motor dynamic model.

1) *DC Motor* : For the mechatronic design of the proposed ventilator, a DC motor is used to provide rotatory motion to the mechanism of the system. The dynamic model of the DC motor is derived from the application of the Kirchoff laws for the electrical part and the rotational equilibrium equations for the shaft, the dynamic model of the system is depicted in Fig. 4.

$$\begin{aligned}\dot{\omega} &= -\frac{B}{J}\omega + \frac{k_2}{J}i \\ \dot{i} &= -\frac{k_1}{L}\omega - \frac{R}{L}i + \frac{1}{L}u\end{aligned}\quad (1)$$

where u , is the input voltage source, which is produced by the robust control system, J is the moment of inertia of the rotor, B is motor viscous friction constant, R is the electric resistance, L is the electric inductance, k_1 is the electromotive force constant and k_2 is the motor torque constant. Then in order to apply a super-twisting control algorithm as will be described in section III, system (1) is transformed into the so-called regular form.

Definition 1: Nonlinear system regular form; a nonlinear system is said to be described into the regular form, if it can be represented, after a possible transformation (diffeomorphism) [12] into the following structure

$$\begin{aligned}\dot{x}_1 &= f_1(x_1, x_2) \\ \dot{x}_2 &= f_2(x_1, x_2) + g_1(x_1, x_2)u_1 \\ y &= h(x_1)\end{aligned}\quad (2)$$

It is important to notice that the electrical part of the system (1) has a much faster dynamic response than their mechanical part, therefore after the proper transformation and considering that $L \ll R \approx 0$. System (1) can be rewritten into the so-called regular form as

$$\begin{aligned}\dot{x}_1 &= x_2 \\ \dot{x}_2 &= f(x)x_2 + g(x)u + D \\ y &= x_1;\end{aligned}\quad (3)$$

Considering the state vector $x = [\theta \ \omega]^T$, $f(x) = \frac{-BR - k_1 k_2}{RJ}$, $g(x) = \frac{k_2}{RJ}$ and u being the motor input voltage. For the controller design it is consider to have unmodelled dynamics, external disturbances and parametric uncertainties which are considered to be lumped into the term D which can be rejected via the control input. Additionally it is worth remarking that after the transformation of system (1) into their regular form (3), the system has a relative degree one with respect to the output $y = x_2$ and relative degree two with respect to the output $y = x_1$ in \mathbb{R}^2 [13].

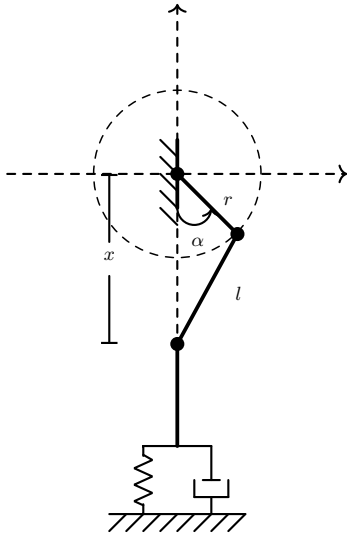


Fig. 5: Slider crank mechanism.

2) *Slider-Crank Mechanism*: Consider the mechanism as shown in Fig. 5, derived from the cosines law it is possible to state that

$$l^2 = r^2 + x^2 - 2lx \cos \alpha \quad (4)$$

from (4) and solving for x it follows that

$$\begin{aligned} l^2 - r^2 &= x^2 - 2rx \cos \alpha \\ &= x^2 - x(2r \cos \alpha) + (r \cos \alpha)^2 - (r \cos \alpha)^2 \\ &= (x - r \cos \alpha)^2 - (r \cos \alpha)^2 \end{aligned} \quad (5)$$

Therefore the position of the final effector of the slider is given by

$$x = r \cos \alpha + \sqrt{l^2 - r^2 \sin^2 \alpha} \quad (6)$$

and the velocity of the slider with respect to the crank angle is described by

$$\dot{x} = -r \sin \alpha - \frac{r^2 \sin \alpha \cos \alpha}{\sqrt{l^2 - r^2 \sin^2 \alpha}} \quad (7)$$

It is worth mentioning that there is a gearbox connected to the shaft of the motor that has a ration of 1:103 reducing the speed to around 80 RPM. This gearbox has an output shaft which is connected to a pair of helical gears with a relation 3:5 to further reduce the output speed and increase the torque to 48 RPM. This done for 2 purposes: 1.- to approach the maximum speed to the maximum respiratory frequency, which is around 30 inhalations per minute, and 2.- to increase the torque and avoid complications with the ventilator's negative pressure. The gears are helical to reduce the noise, vibration, and increase output power.

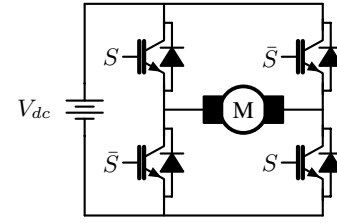


Fig. 6: Proposed H bridge configuration.

D. Power Electronics

The power electronics interface for the DC motor allows the switching with an external 12 v power supply, this is done by means of a set of MOSFET transistors in their H-bridge configuration, as shown in Fig. 6. Where the H-bridge activation signals are generated through PWM (S, \bar{S}) modulation, which is implemented by software using Simulink®.

III. NONLINEAR ROBUST CONTROL

In this section, the proposed control scheme for volume tidal flow regulation for the designed artificial ventilator is presented. For this purpose, the super-twisting sliding mode control algorithm background theory explained.

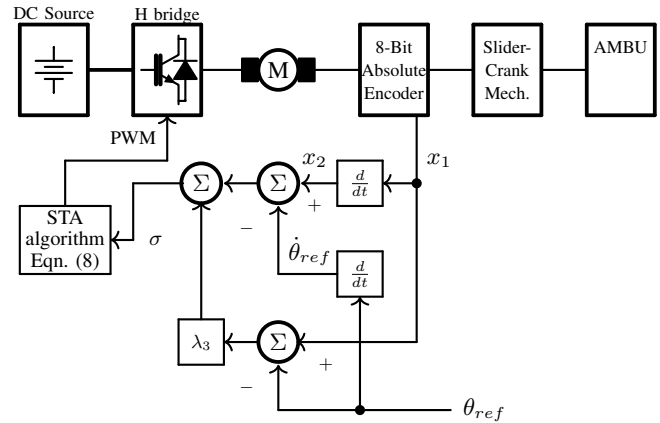


Fig. 7: Proposed artificial Ventilator Control System Configuration.

A. Sliding Mode Super-Twisting Controller

Sliding mode control is considered to be a nonlinear control scheme, that has certain characteristics of interest for the design of robust controllers, among them are the relative simplicity of design, the invariance to system dynamic characteristics and external perturbations, a wide range of operational modes such as regulation and trajectory tracking control [14]. The super-twisting algorithm (STA) is a second-order sliding mode controller and is principally used for systems with principal dynamics of relative degree one [15]. The STA is defined as the sum of two terms as follows

$$\begin{aligned} u_{st} &= -\lambda_1 |\sigma|^{1/2} \text{sign}(\sigma) + u_1 \\ \dot{u}_1 &= -\lambda_2 \text{sign}(\sigma) \end{aligned} \quad (8)$$

Where $\lambda_1, \lambda_2 > 0$, are design parameters, σ is the sliding surface. For the application proposed in this work, it is required to perform time-varying trajectory tracking control, for the STA (8), the following sliding surface σ is defined as seen in [16], using a control configuration as seen in Fig. 7.

$$\sigma = (x_2 - \omega_{ref}) + \lambda_3(x_1 - \theta_{ref}) \quad (9)$$

Remark 1: It is worth-remarking that the proposed control scheme (8) is a robust controller in the sense of rejection of disturbances and with the proper selection of the sliding surface σ the STA does not depend on the parameters of the model, only the knowledge of the state variables $[\omega, \theta]$ (which are accessible through an encoder) and the reference to follow. Similarly, the Super-Twisting controller has a continuous signal as control action, unlike a first-order sliding mode controller, where a high-frequency switched signal would be used as a control action. Finally, the chattering phenomenon is considerably reduced.

IV. SIMULATION AND EXPERIMENTAL RESULTS

In this section, the simulation results obtained from the mechanical modeling of the system are presented as well as the experimental results for the artificial ventilator prototype are presented. Both simulation and experimental results were carried out by using MATLAB/Simulink®.

TABLE I: Artificial Ventilator Dimensions

Parameter	Measure
Height	453.8 mm
Width	260 mm
Depth	250 mm
Crank	32 mm
Connecting rod	100 mm
Slider	186 mm

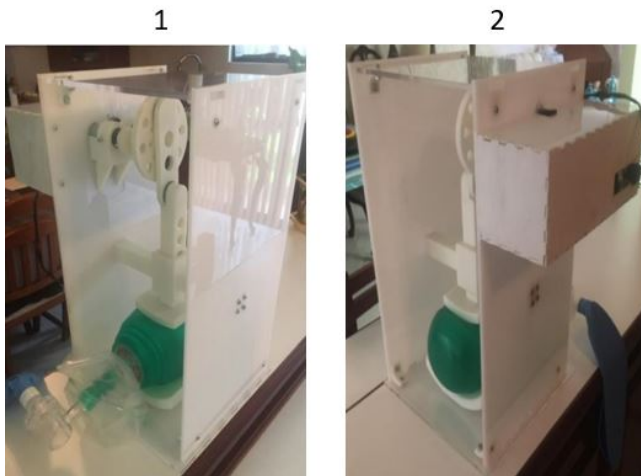


Fig. 8: Artificial breathing machine prototype.

Fig. 8 shows the physical construction and implementation of the proposed and designed artificial ventilator based on

3D printing, it is important to mention that the proposed design is based on a design for manufacture and assembly (DFMA), which means the design for ease of manufacture of the ventilator. The lengths of the links of the slider-crank mechanism as well as the dimensions of the proposed design are shown in Table I.

Fig. 9 depicts the control box, that includes the micro-controller which is an Arduino Due®, an H-Bridge, and an absolute 8-bit Encoder to measure the angular position of the motor. The mentioned set of components is controlled by the software Simulink®, which allows the design and testing of algorithms and their soft-real-time implementation into the embedded microcontroller. The main advantage of this type of configuration is that makes this proposal capable of following different breathing cycles in a robust and constant way.

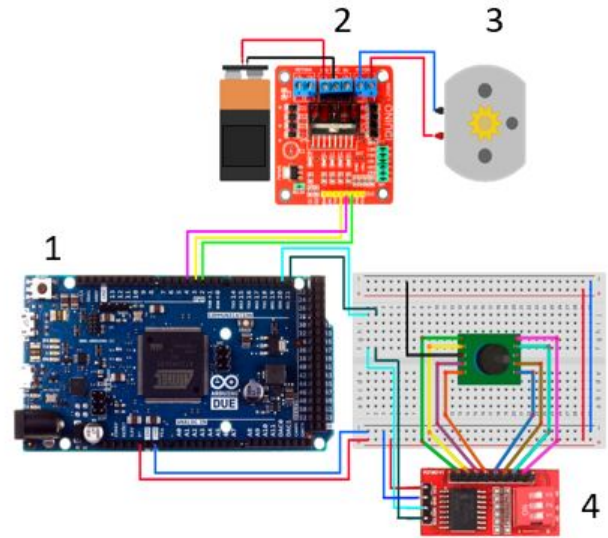


Fig. 9: Embedded micro controller and power electronics. 1. Arduino Due, 2. H bridge, 3. DC motor, 4. Encoder

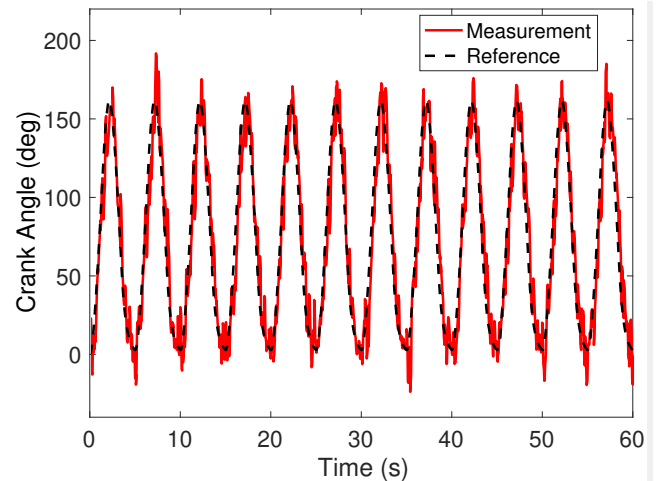


Fig. 10: Crank angle measurement.

Fig. 10 depicts the trajectory tracking control for the crank, by means of the sliding modes controller (8), with the parameters $\lambda_1 = 100$, $\lambda_2 = 0.1$ and $\lambda_3 = 3$ and the proposed sliding surface (9). The tracking profile consists of a trajectory of 0° to 180° degrees, corresponding to half a revolution of the crank, which produces a compression cycle of the AMBU. Notice that the frequency of the reference signal was chosen in order to perform 12 breathing cycles per minute, a parameter which was chosen for experimental purposes, the repertory frequency can be adjusted for the requirements of specific patients. To avoid a position of collinearity between the crank and connecting rod links, the rotation cycle was chosen from 0° to 160° . The obtained results demonstrate the effectiveness of the STA with the selected sliding surface (9) for controlling the angular position of the crank, despite the relative degree of the system in relation to the output, and the rejection of the unmodeled dynamics of the system as the AMBU compression cycle and parameter uncertainties.

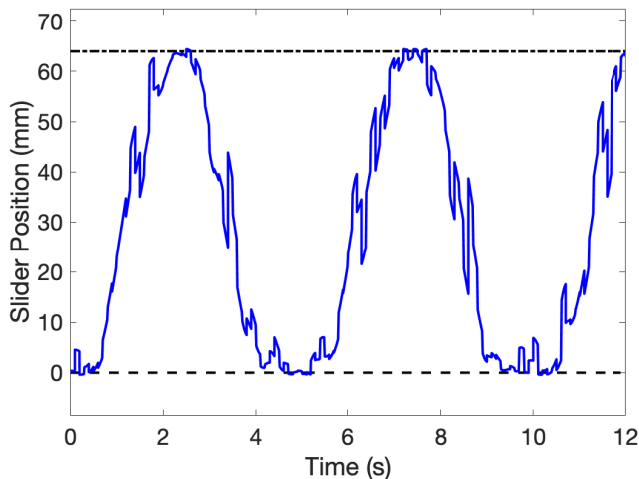


Fig. 11: Slider position.

Fig. 11 shows the slider position measured from the bottom of the ventilator, it is important to mention that for design purposes the zero position of the slider is considering to be at 6 mm from the bottom of the ventilator, this is in order to avoid the full compression of the AMBU and avoid damage. It is possible to appreciate at Fig. that when the slider link is at 0 mm it represents the full compression of the AMBU, that is when the slider-crank mechanism is at its full displacement. Then when the slider is at 64 mm represents the expansion of the AMBU bag. It is important to mention that this harmonic movement of the machine regulates the tidal volume flow which is delivered to the patient, following the phases of the ventilation cycle as seen in Fig.1.

V. CONCLUSIONS

This work proposes the design of a low-cost artificial ventilator in which mechatronic design strategies and manufacturing techniques based on rapid prototyping were implemented. To guarantee the robustness and effectiveness of

the proposed design, a robust control scheme based on a sliding mode super-twisting controller is used which allows the proper trajectory tracking control and enables to follow the required respiratory profiles. Simulation and experimental results validate the effectiveness of the proposed controller and mechatronic design. As future development, it is proposed to work toward the grant of the certification of this prototype in order to be used in the medical sector.

REFERENCES

- [1] D. J. Baker, *Artificial Ventilation, a Basic Clinical Guide*. Springer, 2016.
- [2] S. Nava and F. Fanfulla, *Non Invasive Artificial Ventilation; How, When and Why*. Springer-Verlag Italy, 2010.
- [3] M. Warner and B. Patel, *Mechanical Ventilation*, 12 2013, pp. 981–997.e3.
- [4] I. Jenayeh, F. Simon, S. Bernhard, H. Rake, and B. Schaible, “Digital control of a positioning device for a ventilation machine,” in *1997 European Control Conference (ECC)*, July 1997, pp. 2341–2346.
- [5] A. Das, P. P. Menon, J. G. Hardman, and D. G. Bates, “Optimization of mechanical ventilator settings for pulmonary disease states,” *IEEE Transactions on Biomedical Engineering*, vol. 60, no. 6, pp. 1599–1607, 2013.
- [6] Hoi-Fei Kwok, D. A. Linkens, M. Mahfouf, and G. H. Mills, “Siva: a hybrid knowledge-and-model-based advisory system for intensive care ventilators,” *IEEE Transactions on Information Technology in Biomedicine*, vol. 8, no. 2, pp. 161–172, 2004.
- [7] M. R. Islam, M. Ahmad, M. S. Hossain, M. Muinul Islam, and S. F. Uddin Ahmed, “Designing an electro-mechanical ventilator based on double cam integration mechanism,” in *2019 1st International Conference on Advances in Science, Engineering and Robotics Technology (ICASERT)*, 2019, pp. 1–6.
- [8] Wen Xin-rong, Wang Wei-hua, You Cai-xia, Xie Lu, Li Meng, and Zhang Guang-de, “Dynamic analysis for slider-crank mechanism of engine at the presence of nonlinear friction,” in *2011 International Conference on Electric Information and Control Engineering*, 2011, pp. 2125–2128.
- [9] M. Shahid, “Prototyping of artificial respiration machine using ambu bag compression,” in *2019 International Conference on Electronics, Information, and Communication (ICEIC)*, 2019, pp. 1–6.
- [10] Y. Zhao, R. Qi, and Y. Zhao, “Dimensional synthesis of a slider-crank mechanism based heavy-load positioner,” in *2009 International Conference on Measuring Technology and Mechatronics Automation*, vol. 3, 2009, pp. 59–62.
- [11] Chin-Wen Chuang, Chung-Dar Lee, and Chin-Lang Huang, “Applying experienced self-tuning pid control to position control of slider crank mechanisms,” in *International Symposium on Power Electronics, Electrical Drives, Automation and Motion, 2006. SPEEDAM 2006.*, 2006, pp. 652–657.
- [12] S. Ramos-Paz, F. Ornelas-Tellez, and A. G. Loukianov, “Nonlinear optimal tracking control in combination with sliding modes: Application to the pendubot,” in *2017 IEEE International Autumn Meeting on Power, Electronics and Computing (ROPEC)*, 2017, pp. 1–6.
- [13] H. K. Khalil, *Nonlinear Systems*. Prentice Hall, 2002.
- [14] W. Perruquetti and J. Barbot, *Sliding Mode Control In Engineering*. Marcel-Dekker, 2002.
- [15] Y. Shtessel, C. Edwards, L. Fridman, and A. Levant, *Sliding Mode Control and Observation*. Birkhauser, 2014.
- [16] M. Guermouche, S. A. Ali, and N. Langlois, “Super-twisting algorithm for dc motor position control via disturbance observer,” in *9th IFAC Symposium of Control of Power and Energy Systems CPES 2015: New Delhi, India*, 2015, pp. 43–48.